Volume 1 | Number 1 | Jan 2013 | Pages 1–100

Polymer Chemistry

www.rsc.org/polymers

ROYAL SOCIETY OF CHEMISTRY

ROYAL SOCIETY OF CHEMISTRY

www.rsc.org/polymers

Polymer Chemistry

Polymer Chemistry

Full Paper

A Rather Facile Strategy for Fabrication of PEGylated AIE Nanoprobes

Qing Wan[a], Ke Wang[b], Huilin Du[a], Hongye Huang[a], Meiying Liu[a], Fengjie Deng[a], Yanfeng Dai[a], Xiaoyong Zhang[a,*] and Yen Wei[b,*]

Fluorescent organic nanoparticles (FNPs) have attracted great research interest for biological sensor, biological imaging and disease treatment. However, preparation of ultrabright FNPs using conventional organic dyes is still challenge for their aggregation caused quenching effect. In this work, we reported for the first time that polyethylene glycol (PEG) and an aggregation induced emission (AIE) dye 2,2'-
10 diaminotetraphenyl ethylene (DATPE) can be facilely conjugated by trimellitic anhydride chloride. Taken advantage of the different reaction activity of anhydride and choloride, anhydride-terminated PEG (ADPEG) was first synthesized through the reaction between hydroxyl groups and benzoyl choloride. And then ADPEG could further react with the amino groups of DATPE. Because of the AIE property of DATPE, these amphiphilic triblock copolymers can self assemble into FNPs (PEG-TPE FNPs) and emit
15 strong blue-green fluorescence in aqueous solution. Cell uptake behavior and cytotoxicity evaluation suggested that PEG-TPE FNPs possessed excellent cytocompatibility and could be facilely uptaken by cells, implying that PEG-TPE FNPs are promising for biomedical applications. More importantly, this method described in this work is rather simple, effective and more importantly can be extended to fabricate many other multifunctional FNPs at large scale for various biomedical applications.

20 1. Introduction

Fluorescence nanoprobes with excellent fluorescence intensity have been proved a high-efficiency tool in the modern bioimaging field.[1-6] As we all know, fluorescence nanoprobes have become hotspots in both basic research and practical
25 applications for their well fabrication and wide application for cell imaging and monitoring the process of living systems. Previously, a number of fluorescent inorganic nanoparticles such as semiconductor quantum dots, Ln ion doped nanomaterials, photoluminescent silicon nanoparticles, fluorescent carbon dots
30 and metallic nanoclusters have been successfully developed for bio/chemsensors over the past few decades.[7-18] Although the advantages of strong fluorescence intensity and limited dosage they have, many inherent drawbacks such as difficult synthesis, potential toxicity due to their accumulation in the
35 reticuloendothelial system, poor biodegradability and hydrophobic entites have been gradually discovered, which will be inevitably limited their development in bioimaging and biomedical domains.[19-22] In the recent years, accompanying with the striking development of organic dyes, the fabrication of
40 fluorescent nanoprobes based on the organic dyes have received increasing attentions.[23-26] Nevertheless, it is still difficult to fabricate ultrabright fluorescent nanoprobes using conventional organic dyes for the notorious aggregation caused quenching (ACQ) effect. Therefore, the development of novel fluorescent
45 organic nanoprobes with could overcome these above described problems of fluorescent inorganic nanoparticles and fluorescent organic nanoparticles (FNPs) based on conventional organic dyes

is still highly desirable.

In recent years, a novel type of organic dyes that can emit
50 much strong fluorescence in aggregate state, while non-fluorescence or relative weak fluroescence in the good solvents have recently attracted great research attentions. This unusual phenomenon was named as aggregation induced emission (AIE), which was first reported by Tang et al in 2001.[27] Because of the
55 unique AIE property, FNPs based on the AIE dyes can be elegantly overcome the ACQ effect of FNPs based on conventional organic dyes. It is therefore, a number of FNPs based on AIE dyes have been recently developed and explored for various biomedical applications.[28-40] On the other hand, many
60 fabrication strategies have been established by our and other groups. For example, we have demonsrated that AIE dye (An18) can be facilely encapsulated by a commercial available surfactant (F127) through hydrophobic interaction between the AIE dyes and the hydrophobic segments of F127. However, the obtained
65 FNPs maybe not stable in diluted solution.[41] On the other hand, ene contained AIE dyes can be incorporated into FNPs through the polymerization methods.[42, 43] However, most of these strategies required inert atmosphere, catalysts and heating. Thus a more facile and effective strategy is urgently required to be
70 developed.

Polyethylene glycol (PEG) is a commercial available hydrophilic polymer with excellent biological properties and has proved to be a widespread supplement in biomediacal application for a long time because of its low toxicity to immune system.[44-50]
75 On the other hand, PEG has also been widely used to modify and

fabricate many nanomaterials for biomedical applications.[51, 52] In this contribution, a rather facile strategy have been developed for fabrication of FNPs with strong fluorescent intensity, excellent water-solubility and biocompatibility based on AIE dye and PEG was reported. The experimental process was described in **Scheme 1**. First, the anhydride-terminated PEG (ADPEG) could be synthesized via the easy esterification reaction between hydrophilic PEG and trimellitic anhydride chloride within 10 min. Afterwards, the AIE dye 2,2'-diaminotetraphenyl ethylene (DATPE) was conjugated with the ADPEG through ring opening reaction between the amino groups of DATPE to prepare the amphiphilic PEG-TPE copolymers. Finally, the amphiphilic PEG-TPE copolymers could self assemble into nanoparticles with diameter of a few hundreds nanometers. Furthermore, according to the cell experiment, the high survival rate of cells after incubating with different concentrations of FNPs well proved their great biocompatibility. Therefore, the preparation of water-dispersible FNPs with strong fluorescence intensity was achieved for their potential application in the biomedical and chem/biosensor fields.
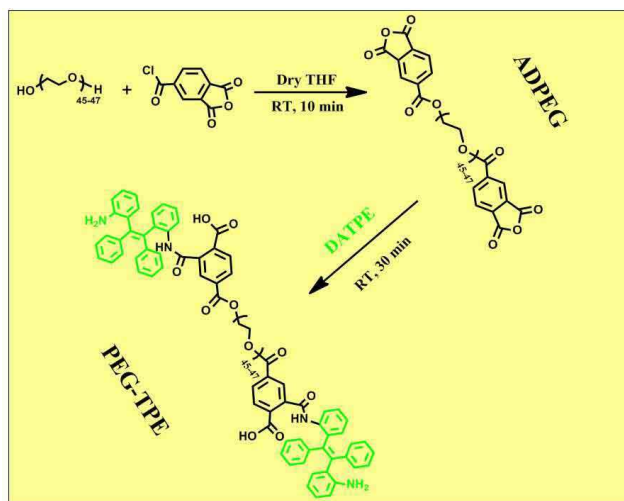
Scheme 1. The schematic procedure for fabricating high water-solubility fluorescence nanoparticles were showed in this picture. The anhydride-terminated PEG was quickly prepared within 10 min via simple and high-efficiency esterification. Afterwards, pre-prepared DATPE AIE dyes were covalently conjugated with the anhydride of PEG via ring-opening reaction.

2. Experiment

2.1 Materials and Characterization

All chemicals were of analytical grade and were used as received without any further purification. Polyethylene glycol (PEG, MW = 2000), trimellitic anhydride chloride (MW = 210.57, 98%) were purchased from Aladdin company (Shanghai China). Zinc powders, titanium tetrachloride, 2-Aminobenzophenone (MW = 197.23, 99.0%) and anhydrous THF were provided from Heowns (Tianjin, China), ammonium chloride and ethyl acetate solution were suffered from Sinopharm Chemical reagents Co., Ltd. (Shanghai, China).

^{1}H NMR spectra was recorded on Bruker Avance-400 spectrometer with D_2O and $CDCl_3$ as the solvent. The synthetic polymers and materials were characterized by Fourier transform infrared spectroscopy (FT-IR) using KBr pellets, FT-IR spectra were supplied from Nicolet5700 (Thermo Nicolet corporation). Transmission electron microscopy (TEM) images were recorded on a Hitachi 7650B microscope operated at 80 kV, the TEM specimens were got by putting a drop of the nanoparticle ethanol suspension on a carbon-coated copper grid. The fluorescence data was obtained from the Fluorescence spectrophotometer (FSP, model: C11367-11), which purchased from Hamamatsu (Japanese).

2.2 Synthesis of DATPE

The DATPE could be mildly synthesized using 2-Aminobenzophenone by typical McMurry reaction as described previously.[53] Briefly, $TiCl_4$ (0.0549 mol, 6 mL) was added dropwise into stirring suspension of zinc powder (0.1098 mol, 7.137 g) in dry tetrahydrofuran (THF) solution (60 mL) at 0 °C for 30 min. After refluxing 2 h at 80 °C under nitrogen atmosphere, 2-Aminobenzophenone (0.0274 mol, 5.4 g) dissolved in 30 mL THF solution was gradually added into above reaction system, which was refluxed for another 8 h. The resulting reactive solution was cooled down to the room temperature and put into 5% ammonium chloride solution and stirring 30 min, the dispersed insoluble white residue was seperated by vacuum filtration. The resulting primary products were obtained by extraction three times using ethyl acetate. After drying with anhydrous magnesium sulfate about 4 h, the solvents were removed by vacuum rotary evaporation. The pure product could be achieved by silica gel with ethyl acetate/n-hexane (1:10, v/v). Yield=52.6%.

2.3 Fabrication of FNPs

The anhydride-terminated PEG could be synthesized by simple and fast esterification reaction between hydroxyl groups of PEG and benzoyl chloride of trimellitic anhydride chloride. In order to guarantee non-water in PEG samples, the water in purchased PEG was removed by azeotropic using toluene under vacuum rotary evaporation three times. The PEG productors (1 mmol, 2 g) were dissolved in the 20 mL anhydrous THF solution in a dried flask. Next, drops of triethylamine solution and trimellitic anhydride chloride (2.5 mmol, 526 mg) in 10 mL dry THF solution was added dropwise into reaction system at room temperature (20 °C). After 10 min, the THF solution was removed via rotary evaporation. And then ADPEG was reacted with DATPE to obtain the finally product (PEG-TPE) via ring-opening reaction. Briefly, ADPEG (0.5 mmol, 1.2 g), DATPE (1.2 mmol, 435 mg) were dissolved in 30 mL anhydrous THF solution and stirring at room temperature for 30 min under ambient atmosphere. The resulting polymers conjugated with TPE dye were undergo purification process via frequently dissolved using ethyl acetate and participated using dry diethyl ether three times.

2.4 Cytotoxicity evaluation of PEG-TPE FNPs

The cell viability of PEG-TPE FNPs on Hela cells was evaluated by cell counting kit-8 (CCK-8) assay. Briefly, cells were put into 96-well microplates at a density of 5×10^4 cells mL^{-1} in 160 μL of respective media containing 10% FBS.[54-56] After 24 h of cell attachment, the cells were incubated with different concentrations of PEG-TPE FNPs (20-100 μg mL^{-1}) for 12 and 24 h. Then

nanoparticles were removed and cells were washed with PBS three times. 10 µL of CCK-8 dye and 100 µL of DMEM cell culture medium were added to each well and incubated for 2 h at 37 °C. Afterward, plates were analyzed using a microplate reader
5 (VictorⅢ, Perkin-Elmer). Measurements of formazan dye absorbance were carried out at 450 nm, with the reference wavelength at 620 nm. The values were proportional to the number of live cells. The percent reduction of CCK-8 dye was compared to controls (cells not exposure to PEG-TPE FNPs),
10 which represented 100% CCK-8 reduction. Three replicate wells were used per microplate, and the experiment was operated for three times. Cell survival was expressed as absorbance relative to that of untreated controls. Results are presented as mean ± standard deviation (SD).

15 **2.5 Confocal microscopic imaging**

Hela cells were cultured in Dulbecco's modified eagle medium (DMEM) supplemented with 10% heat-inactivated FBS, 2 mM glutamine, 100 U mL^{-1} penicillin, and 100 µg mL^{-1} of streptomycin. Cell culture was controlled at 37 °C in a similar
20 humidified condition of 95% air and 5% CO_2 in culture medium. Culture medium should be updated every three days for maintaining the exponential growth of the cells. Before treatment, cells were seeded in a glass bottom dish with a density of 1×10^5 cells per dish. On the day of treatment, the cells were incubated
25 with PEG-TPE FNPs at a final concentration of 10 µg mL^{-1} for 3 h at 37 °C. Afterward, the cells were washed three times with PBS to remove the PEG-TPE FNPs and then fixed with 4% paraformaldehyde for 10 min at room temperature. Cell images were obtained using a confocal laser scanning microscope
30 (CLSM) Zesis 710 3-channel (Zesis, Germany) with the excitation wavelength of 405 nm.

3. Results and discussion

The successful preparation of 2,2'-diaminotetraphenyl ethylene AIE dyes could be judged by ^{1}H NMR spectrum (**Fig. S1**). The
35 results can be analysized in follows. ^{1}H NMR (300 MHz, CDCl$_3$, δ): 4.34-4.87 ppm (d, 2H, -NH$_2$). The other protons existed in benzene ring were located at 6.34-7.83 ppm because of coinciding with CDCl$_3$. The ^{1}H NMR spectra of PEG2000, ADPEG and PEG-TPE were shown in **Fig. 1**. Compared with the
40 spectrum of PEG2000, novel chemical shift at 7.5-8.5 ppm ascribed to the introduction of benzene ring was observed in the sample of ADPEG, implying that the successful conjugated PEG2000 with trimellitic anhydride chloride. On the other hand, the peak located at 1.84 ppm was belonged to –OH existed in
45 PEG2000 samples. Obviously, the disappearance of peak at 1.84 ppm for ADPEG samples, further demonstrating that trimellitic anhydride chloride was cojugated with PEG2000 by a simple esterification reaction. These results suggested that chloride group was successfully reacted with the hydroxyl groups of
50 PEG2000 via rapid esterification reaction. However, no chemical shift signal was observed at 9.87 ppm, suggesting the anhydride group of trimellitic anhydride chloride did not react with the hydroxyl groups of PEG2000. On the other hand, as we can see the ^{1}H NMR spectrum of PEG-TPE copolymers, the new single
55 peak located at 9.87 ppm could be attributed to the chemical shift of –COOH. The appearance of –COOH in the sample of PEG-

TPE demonstrated that the amino groups of DATPE can further react with the anhydride groups of ADPEG via ring-opening reaction. Taken together, we concluded that the PEG-TPE
60 copolymers can be elegantly prepared via conjugating PEG and DATPE using trimellitic anhydride chloride as linkages**.** As compared previous methods for fabrication of AIE dyes based FNPs, this strategy described in this work is rather simple, effective and feasible. The reaction can be occurred at room
65 temperature, air atmosphere and absence of catalysts. Therefore, it is particular useful for fabrication of FNPs at large scale. More importantly, carboxyl groups are introduced in the FNPs, that can be further utilized for further conjugation targeting agents or loading biological activity agents. Therefore, FNPs fabricated by
70 this strategy is potential for fabrication of multifunctional therapeutic nanosystems.
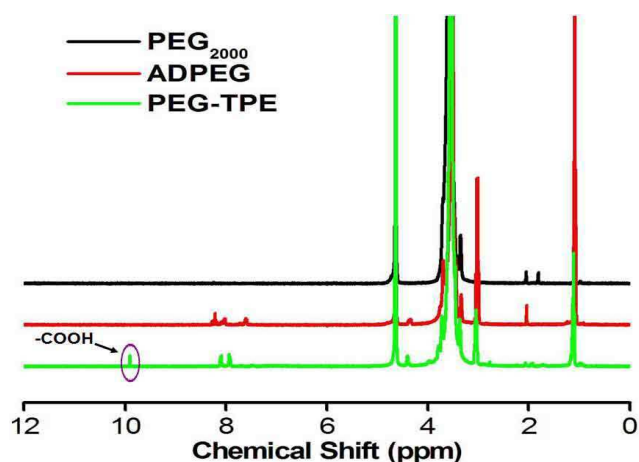

Fig. 1 The ^{1}H NMR spectra of PEG2000, ADPEG and PEG-TPE samples, which demonstrated that successful fabrication of novel FNPs
75 with strong fluorescence and great water-dispersible properties to overcome the drawback of water-insoluble. The chemical shift appeared between 7.5-8.5 ppm, demonstrating that successful esterification reaction between PEG and trimellitic anhydride chloride. On the other hand, the new chemical shift at 9.87 ppm could be ascribed to the –COOH,
80 suggesting that DATPE was perfectly conjugated with ADPEG.

The successful formation of PEG-TPE FNPs could also be confirmed by FT-IR. As shown in **Fig. 2**, comparing with samples of PEG2000, the new characterized peak located at 1732 cm^{-1} was observed in the samples of ADPEG, which was
85 attributed to the stretching vibration of the C=O groups belonged to the anhydride. Furthermore, a series of new peaks appeared between 1300 and 1500 cm^{-1} can be ascribed to the stretching vibration of aromatic ring. These results suggested that anhydride ring were combined with PEG2000. After DATPE was
90 suspended the side chains of ADPEG via ring-opening reaction, a strong stretching vibration of –NH$_2$ shown at 3410 cm^{-1} was observed in samples of PEG-TPE FNPs. On the other hand, two characterized peaks respectively centered at 1680 cm^{-1} and 1630 cm^{-1} could be considered as the stretching vibration of the C=O
95 of amide and carboxyl groups, which were formed after ring-opening reaction. More importantly, these results provided direct evidence that successful fabrication of AIE dye based FNPs with strong fluorescence and water-dispersible properties.
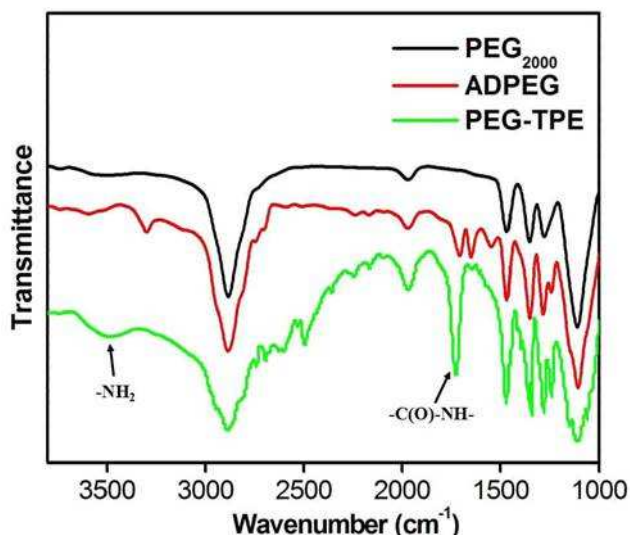
Fig. 2 FT-IR spectra of PEG2000, ADPEG and PEG-TPE samples, which provided evidence of successful formation of PEG-TPE FNPs.

In order to determine the state of PEG-TPE nanoparticles in water, the absorption of FNPs was detected by UV-Vis spectrum. As shown in Fig. 2, the entire spectrum began to increase when wavelength located at 350 nm, which provided evidence that PEG-TPE particles was formed in the water solution. These dispersed FNPs effectively decrease the light transmission and cause the obvious light absorption, which evidenced that the hydrophobic dyes was successfully modified by hydrophilic polymers and thus obtained FNPs were well dispersed in water solution (Fig. S2). The unique AIE characterization of DATPE was also evaluated by adjusting different volume of water in water/THF mixture. As shown in Fig. S3A, the emission of DATPE was special weak when 10 µM DATPE was dissolved in THF solution, suggesting that excellent AIE performance with weak fluorescence in good solvents. However, accompanying with the increase of water fraction, the fluorescent intensity was slowly enhanced before volume ratio of water/THF up to 7:3. Afterwards, the fluorescent intensity was enhanced swiftly until the water fraction up to 90%. Therefore, these interesting phenomenon suggested the unique aggregation-enhanced emission characterization of DATPE. On the other hand, the variation trend of DATPE FL intensity was also evaluated. As we can see from the Fig. S3B, the stable increase of fluorescent intensity with the enhanced of water fraction demonstrated that water is poor solvents for DATPE dyes. the phenomenon of FL increasing could be explained that DATPE dyes were aggregated in water solution and emitted strong luminescence.

Because of the amphiphilic properties, PEG-TPE copolymers can self assemble into core-shell micelles in aqueous solution. In which, the PEG segments were expanded into water and AIE dye was encapsulated in the core. Thus the obtained PEG-TPE FNPs displayed good water dispersibility and exhibited strong blue-green fluorescence in pure water. The successful formation of water dispersible nanoparticles are first confirmed by the photoimages. It can be seen that PEG-TPE FNPs can be well dispersed in aqueous solution and no aggregation is observed (**Fig. S4**). No precipitation was observed even after this suspension was deposited for more than several days, confirming

the excellent water dispersibility of PEG-TPE FNPs. The self assembly of PEG-TPE into nanoparticles in aqueous solution can be also evidenced by the fluorescent images of PEG-TPE FNP suspension (**Fig. S4**). Blue-green fluorescence can be seen from PEG-TPE FNP suspension after it was irradiated by UV-lamp at 365 nm. The uniform fluorescence further indicated that the successful synthesis of PEG-TPE copolymers. The detailed information about fluorescence of PEG-TPE FNPs was displayed in **Fig. 3**. The maximum emission wavelength of PEG-TPE FNPs in water was located at 471 nm, while the fluorescence excitation wavelength of FNPs appeared at 330 nm. Fluoresence quantum yield is a very important fluorescent property. The fluorescence quantum yield of PEG-TPE FNPs is as high as 18.9% using quinine sulfate as the reference dye. The high fluorescence quantum yield of PEG-TPE FNPs make them promising for bioimaging applications. The fluorescence stability of PEG-TPE FNPs has also examined. It can be seen that the maximum emission fluorescent intensity value of PEG-TPE FNPs is 468.3. After the suspension was continuously irradiated using UV lamp (365 nm) for 1 h, the maximum emission fluorescent intensity value is 405.3 (**Fig. S5**). These results suggested that the PEG-TPE FNPs have high fluorescence quantum yield and excellent fluorescence stability.
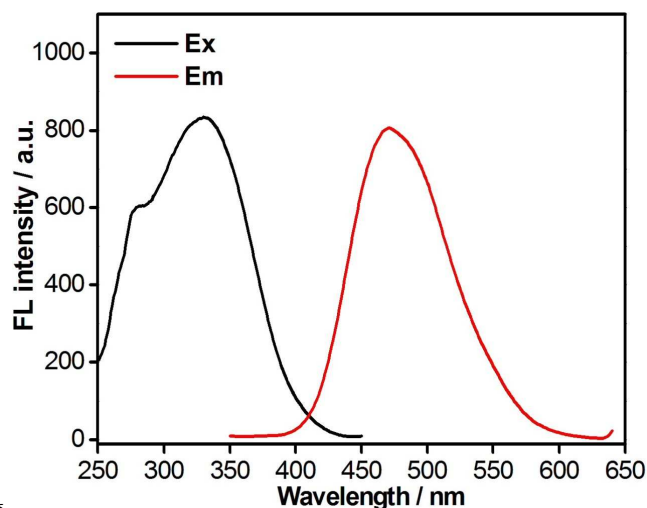

Fig. 3 The fluorescence spectrum of PEG-TPE samples dispersed in water.

The size and morphology of PEG-TPE FNPs was characterized by TEM, which also evidenced that successful preparation of FNPs based on TPE. As shown in **Fig. 4**, the diameter of most PEG-TPE FNPs was falled in the range of 100-300 nm. The size distribution of PEG-TPE FNPs was calculated based on the TEM images. Our results suggested that the size distribution of PEG-TPE FNPs is 205 ± 28.5 nm. The possible mechanism for forming spherical FNPs of PEG-TPE could be explained that hydrophobic segments (TPE) were insoluble and curled into sphere in water. Meanwhile, the hydrophilic segments (PEG) were covered on the surface of hydrophibic core and contacted with water, resulting in excellent water-dispersable property of PEG-TPE FNPs. Furthermore, the hydrodynamic size of PEG-TPE FNPs was determined by dynamic light scattering (DLS). The PEG-TPE FNPs were dispersed in water at a concentration about 0.5 mg mL^{-1}. Results suggested that the hydrodynamic size

of PEG-TPE FNPs is 296.6 ± 112.8 nm. And norrow polydispersity with polydispersity index (PDI = 0.232) (Fig. S6). All the above results suggested that the PEG-TPE FNPs with suitable size and excellent dispersibility in aqueous solution, 5 impling their potential for biomedical applications.
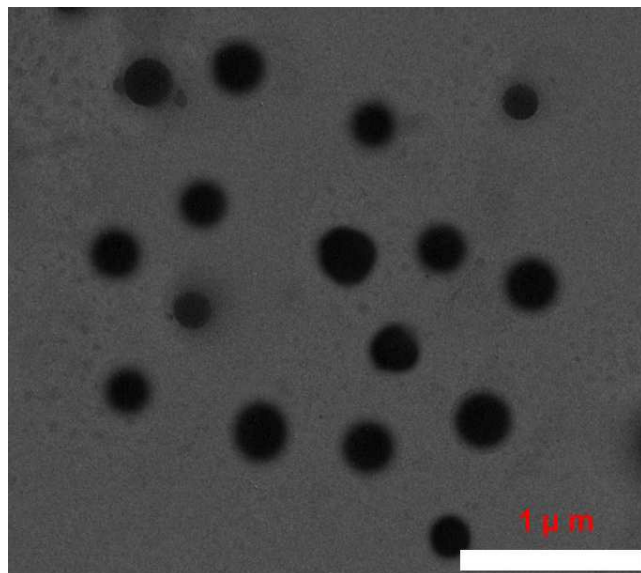

Fig. 4 TEM image of PEG-TPE FNPs, scale bar = 1 μm. It can be seen that many spherical aggregation particles with diameter about few hundred nanomaters can be observed.

10 Biocompatibility is essential for the biomedical applications of biomaterials.[57, 58] In this work, the preliminary biocompatibility evaluation was conducted using CCK-8 assay, which has been previously adopted for evaluating the effect of the biomaterials on the cell viability. The cell viability values of Hela cells after 15 they were incubated with different concentrations of PEG-TPE FNPs for both 12 and 24 h were displayed in **Fig. 5**. No significant cell viability changes can be observed. Even at high concentrations (e.g. 100 μg mL^{-1}) for 24 h, the cell viability values are still greater than 95%. These results confirmed that 20 PEG-TPE FNPs possess excellent biocompatibility and negative toxicity toward cells. As compared with the commonly used fluorescent nanoprobes (e.g. semiconductor quantum dots), the PEG-TPE FNPs should be more suitable for biomedical applications for their high water dispersibility, excellent 25 biocompatibility and potential biodegradability.
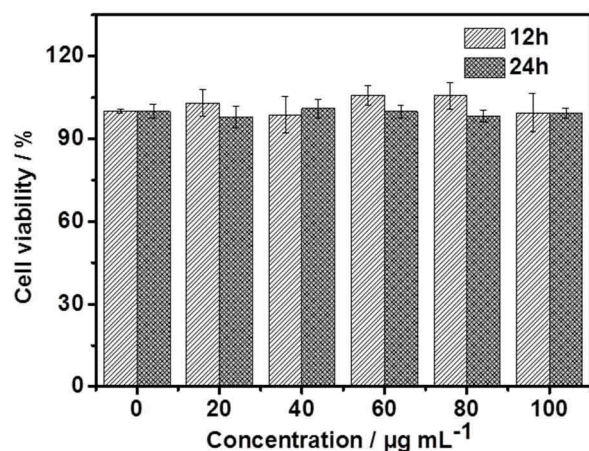

Fig. 5 The biocompatibility evaluation of Hela cell after incubating with different concentrations (0-100 μg mL^{-1}) of PEG-TPE FNPs. The curve of Hela cell viability after incubating with a series of concentrations of FNPs 30 for 12 and 24 h. The cell evaluation experiment suggested that FNPs showed negative toxicity to cells.

The cell uptake behavior of PEG-TPE FNPs was evaluated by CLSM. As shown in the **Fig. 6**, strong fluorescence sign was observed after cells were incubated with 10 μg mL^{-1} of PEG-TPE 35 FNPs for 3 h. On the other hand, some areas with relative weak fluorescence or almost no fluorescence can be also observed (**Fig. 6A**). These areas should be the location of cell nucleus. These results suggested that PEG-TPE FNPs can be internalized by cells and mainly distributed in cytoplasm. on the other hand, due to the 40 size of PEG-TPE is obviously large than that of nucleus pore. The PEG-TPE FNPs is immposible entered into cell nucleus. On the other hand, we found that cells still kept their normal morphology after incubated with PEG-TPE FNPs, further confirming the excellent biocompatibility of PEG-TPE FONs (**Fig. 6B**). 45 combination of the water dispersibility, biocompatibility and strong fluorescence, the obtained PEG-TPE FNPs are expected very promising candidates for cell imaging and many other biomedical applications. Although many strategies have been developed for fabrication of AIE dye based nanoprobes, most of 50 these methods are involved in complex experimental procedure, time consuming, inert gas protection and catalysts. As compared with previous strategies, the method described in this work is rather simple, fast and effective. The reaction involved in this method can be occurred at room temperature, air atmosphere 55 within 1 h and without needing catalysts. Therefore it is potential for preparation of AIE dye based FNPs at large scale, which therefore should be of great importance for their applications.
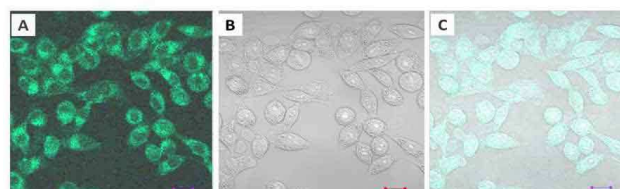

Fig. 6 Cell imaging of PEG-TPE nanoparticles with 10 μg mL^{-1} using 60 CSLM. (A) exciting at 405 nm. (B) bright fields. (C) the combination of images of A and B.

Conclusion

In summary, a rather facile method for fabrication of AIE-based FNPs with excellent biocompatibility, great water-dispersibility 65 and fluorescence properties via covalent combination of AIE dye (DATPE) and PEG was developed. Taken advantage of the difference reaction activity of trimellitic anhydride chloride toward DATPE and ADPEG, this strategy can elegantly conjugated the hydroxyl groups of PEG and the amino groups of 70 DATPE. The reactive conditions in this work is especially simple and efficient, including ambient temperature, catalyst-free, short reactive time and without protection gases at large scale. More importantly, because of the existence of carboxyl groups in the end of AIE FNPs, it provides multifunctional platform for the 75 introduction of many other components including drugs and targeting agents to the AIE FNPs, which would have a profound impact for the biomedicine fields. Therefore, considering their

superior performance, thus synthetic FNPs would have wide application prospects for the biosensor and biomedical fields.

Acknowledgements

Notes

[a] Department of Chemistry and Jiangxi Provincial Key Laboratory of New Energy Chemistry, Nanchang University, 999 Xuefu Avenue, Nanchang 330031, China. [b] Department of Chemistry and the Tsinghua Center for Frontier Polymer Research, Tsinghua University, Beijing, 100084, P. R. China.
xiaoyongzhang1980@gmail.com; weiyen@tsinghua.edu.cn.
† Electronic Supplementary Information (ESI) available: [¹H NMR of DATPE, photostability of PEG-TPE FNPs, hydrodyanmic size of PEG-TPE FNPs and AIE property of DATPE.]. See DOI: 10.1039/b000000x/

References

1. A. Burns, H. Ow and U. Wiesner, *Chem. Soc. Rev.*, 2006, **35**, 1028-1042.
2. X. Zhang, X. Zhang, B. Yang, Y. Zhang and Y. Wei, *ACS Appl. Mater. Inter.*, 2014, **6**, 3600-3606.
3. Y. Yang, F. An, Z. Liu, X. Zhang, M. Zhou, W. Li, X. Hao, C. s. Lee and X. Zhang, *Biomaterials*, 2012, **33**, 7803-7809.
4. M. Liu, J. Ji, X. Zhang, X. Zhang, B. Yang, F. Deng, Z. Li, K. Wang, Y. Yang and y. wei, *J. Mater. Chem. B*, 2015, **3**, 3476 - 3482.
5. J. Hui, X. Zhang, Z. Zhang, S. Wang, L. Tao, Y. Wei and X. Wang, *Nanoscale*, 2012, **4**, 6967-6970.
6. X. Zhang, S. Wang, M. Liu, B. Yang, L. Feng, Y. Ji, L. Tao and Y. Wei, *Phys. Chem. Chem. Phys.*, 2013, **15**, 19013-19018.
7. L. Basabe Desmonts, D. N. Reinhoudt and M. Crego Calama, *Chem. Soc. Rev.*, 2007, **36**, 993-1017.
8. Y. Dong, R. Wang, G. Li, C. Chen, Y. Chi and G. Chen, *Anal. Chem.*, 2012, **84**, 6220-6224.
9. X. Gao, Y. Cui, R. M. Levenson, L. W. Chung and S. Nie, *Nat. Biotechnol.*, 2004, **22**, 969-976.
10. B. A. Kairdolf, A. M. Smith, T. H. Stokes, M. D. Wang, A. N. Young and S. Nie, *Annu. Rev. Anal. Chem.*, 2013, **6**, 143.
11. Z. Li and E. Ruckenstein, *Nano. Lett.*, 2004, **4**, 1463-1467.
12. J. M. Liu, L. p. Lin, X. X. Wang, S. Q. Lin, W. L. Cai, L. H. Zhang and Z. Y. Zheng, *Analyst*, 2012, **137**, 2637-2642.
13. H. Ow, D. R. Larson, M. Srivastava, B. A. Baird, W. W. Webb and U. Wiesner, *Nano lett.*, 2005, **5**, 113-117.
14. I. Roy, T. Y. Ohulchanskyy, D. J. Bharali, H. E. Pudavar, R. A. Mistretta, N. Kaur and P. N. Prasad, *P. Natl. Acad. Sci. USA.*, 2005, **102**, 279-284.
15. J. Shen, Y. Zhu, X. Yang and C. Li, *Chem. Commun.*, 2012, **48**, 3686-3699.
16. H. X. Zhao, L. Q. Liu, Z. De Liu, Y. Wang, X. J. Zhao and C. Z. Huang, *Chem.Commun.*, 2011, **47**, 2604-2606.
17. X. Zhang, S. Wang, C. Zhu, M. Liu, Y. Ji, L. Feng, L. Tao and Y. Wei, *J. Colloid Interf. Sci.*, 2011, **397**, 39-44.
18. X. Zhang, J. Hui, B. Yang, Y. Yang, D. Fan, M. Liu, L. Tao and Y. Wei, *Polym. Chem.*, 2013, **4**, 4120-4125.
19. S. Chandra, P. Das, S. Bag, D. Laha and P. Pramanik, *Nanoscale*, 2011, **3**, 1533-1540.
20. Y. P. Ho and K. W. Leong, *Nanoscale*, 2010, **2**, 60-68.
21. X. Wu, X. He, K. Wang, C. Xie, B. Zhou and Z. Qing, *Nanoscale*, 2010, **2**, 2244-2249.
22. A. Shiohara, S. Prabakar, A. Faramus, C. Y. Hsu, P. S. Lai, P. T. Northcote and R. D. Tilley, *Nanoscale*, 2011, **3**, 3364-3370.
23. P. Sharma, S. Brown, G. Walter, S. Santra and B. Moudgil, *Adv. Colloid Interfac.*, 2006, **123**, 471-485.
24. J. Bouffard, Y. Kim, T. M. Swager, R. Weissleder and S. A. Hilderbrand, *Org. lett.*, 2008, **10**, 37-40.
25. M. Liu, X. Zhang, B. Yang, Z. Li, F. Deng, Y. Yang, X. Zhang and Y. Wei, *Carbohyd. Polym.*, 2015, **121**, 49-55.
26. M. Liu, X. Zhang, B. Yang, F. Deng, J. Ji, Y. Yang, Z. Huang, X. Zhang and Y. Wei, *RSC Adv.*, 2014, **4**, 22294-22298.
27. J. Luo, Z. Xie, J. W. Y. Lam, L. Cheng, H. Chen, C. Qiu, H. S. Kwok, X. Zhan, Y. Liu, D. Zhu and B. Z. Tang, *Chem. Commun.*, 2001, **37**, 1740-1741.
28. Q. Qi, Y. Liu, X. Fang, Y. Zhang, P. Chen, Y. Wang, B. Yang, B. Xu, W. Tian and S. X.-A. Zhang, *RSC Adv.*, 2013, **3**, 7996-8002.
29. P. Alam, P. Das, C. Climent, M. Karanam, D. Casanova, A. Choudhury, P. Alemany, N. Jana and I. Laskar, *J. Mater. Chem. C*, 2014, **2**, 5615-5628.
30. Y. Chen, J. W. Lam, S. Chen and B. Z. Tang, *J. Mater. Chem. C*, 2015, **2**, 6192-6198.
31. Y. Gao, Y. Qu, T. Jiang, H. Zhang, N. He, B. Li, J. Wu and J. Hua, *J. Mater. Chem. C*, 2014, **2**, 6353-6361.
32. L. Kong, Y.-p. Tian, Q.-y. Chen, Q. Zhang, H. Wang, D.-q. Tan, Z.-m. Xue, J.-y. Wu, H.-p. Zhou and J.-x. Yang, *J. Mater. Chem. C*, 2015, **3**, 570-581.
33. Y. Lin, G. Chen, L. Zhao, W. Z. Yuan, Y. Zhang and B. Z. Tang, *J. Mater. Chem. C*, 2015, **3**, 112-120.
34. G. Yu, G. Tang and F. Huang, *J. Mater. Chem. C*, 2014, **2**, 6609-6617.
35. X. Zhang, X. Zhang, L. Tao, Z. Chi, J. Xu and Y. Wei, *J. Mater. Chem. B*, 2014, **2**, 4398-4414.
36. X. Zhang, K. Wang, M. Liu, X. Zhang, L. Tao, Y. Chen and Y. Wei, *Nanoscale*, 2015, 10.1039/C1035NR01444A.
37. Y. Zhang, Y. Chen, X. Li, J. Zhang, J. Chen, B. Xu, X. Fu and W. Tian, *Polym. Chem.*, 2014, **5**, 3824-3830.
38. R. Hu, N. L. Leung and B. Z. Tang, *Chem. Soc. Rev.*, 2014, **43**, 4494-4562.
39. K. Li and B. Liu, *Chem. Soc. Rev.*, 2014, **43**, 6570-6597.
40. H. Lu, X. Zhao, W. Tian, Q. Wang and J. Shi, *RSC Adv.*, 2014, **4**, 18460-18466.
41. X. Zhang, X. Zhang, S. Wang, M. Liu, L. Tao and Y. Wei, *Nanoscale*, 2013, **5**, 147-150.
42. X. Zhang, X. Zhang, B. Yang, J. Hui, M. Liu, Z. Chi, S. Liu, J. Xu and Y. Wei, *Polym. Chem.*, 2014, **5**, 683-688.
43. X. Zhang, X. Zhang, B. Yang, M. Liu, W. Liu, Y. Chen and Y. Wei, *Polym. Chem.*, 2014, **5**, 356-360.
44. Y. H. Choi, F. Liu, J. S. Kim, Y. K. Choi, J. S. Park and S. W. Kim, *J. Control. Release*, 1998, **54**, 39-48.
45. R. Gref, A. Domb, P. Quellec, T. Blunk, R. Müller, J. Verbavatz and R. Langer, *Adv. Drug. Deliver. Rev.*, 2012, **64**, 316-326.
46. A. S. Hoffman, *Adv. Drig. Deliver. Rev.*, 2012, **64**, 18-23.
47. H. Otsuka, Y. Nagasaki and K. Kataoka, *Adv. Drug deliver. Rev.*, 2012, **64**, 246-255.
48. M. Roberts, M. Bentley and J. Harris, *Adv. Drug deliver. Rev.*, 2012, **64**, 116-127.
49. J. Nicolas, S. Mura, D. Brambilla, N. Mackiewicz and P. Couvreur, *Chem. Soc. Rev.*, 2013, **42**, 1147-1235.
50. X. Zhang, X. Zhang, B. Yang, S. Wang, M. Liu, Y. Zhang, L. Tao and Y. Wei, *RSC Adv.*, 2013, **3**, 9633-9636.
51. X. Zhang, S. Wang, C. Fu, L. Feng, Y. Ji, L. Tao, S. Li and Y. Wei, *Polym. Chem.*, 2012, **3**, 2716-2719.
52. X. Zhang, C. Fu, L. Feng, Y. Ji, L. Tao, Q. Huang, S. Li and Y. Wei, *Polymer*, 2012, **53**, 3178-3184.
53. M. P. Aldred, C. Li and M. Q. Zhu, *Chem-Eur. J.*, 2012, **18**, 16037-16045.
54. X. Zhang, W. Hu, J. Li, L. Tao and Y. Wei, *Toxicol. Res.*, 2012, **1**, 62-68.
55. X. Zhang, M. Liu, X. Zhang, F. Deng, C. Zhou, J. Hui, W. Liu and Y. Wei, *Toxicol. Res.*, 2015, **4**, 160-168.
56. X. Zhang, S. Wang, M. Liu, J. Hui, B. Yang, L. Tao and Y. Wei, *Toxicol. Res.*, 2013, **2**, 335-342.
57. J. Yin, C. Kang, Y. Li, Q. Li, X. Zhang and W. Li, *Toxicol. Res.*, 2014, **3**, 367-374.
58. X. Zhang, J. Yin, C. Peng, W. Hu, Z. Zhu, W. Li, C. Fan and Q. Huang, *Carbon*, 2011, **49**, 986-995.